LETTERS

Optical coherent state discrimination using a closed-loop quantum measurement

Robert L. Cook[1], Paul J. Martin[1] & J. M. Geremia[1]

Quantum mechanics hinders our ability to determine the state of a physical system in two ways: individual measurements provide only partial information about the observed system (because of Heisenberg uncertainty), and measurements are themselves invasive—meaning that little or no refinement is achieved by further observation of an already measured system[1]. Theoretical methods have been developed to maximize the information gained from a quantum measurement while also minimizing disturbance[2–4], but laboratory implementation of optimal measurement procedures is often difficult. The standard class of operations considered in quantum information theory[5] tends to rely on superposition-basis and entangled measurements[6], which require high-fidelity implementation to be effective in the laboratory[7]. Here we demonstrate that real-time quantum feedback[8–10] can be used in place of a delicate quantum superposition, often called a 'Schrödinger cat state', to implement an optimal quantum measurement for discriminating between optical coherent states[11,12]. Our procedure actively manipulates the target system during the measurement process, and uses quantum feedback to modify the statistics of an otherwise sub-optimal operator to emulate the optimal cat-state measurement. We verify a long-standing theoretical prediction[13] and demonstrate feedback-mediated quantum measurement[10,14] at its fundamental quantum limit over a non-trivial region of parameter space.

In this work we consider a single mode optical field $\hat{a}$ prepared at random into one of two pure coherent states, $|0\rangle$ or $|\alpha\rangle$, with a priori probabilities $P_0(0)$ and $P_0(\alpha)$. Privy only to the candidate states and their likelihoods, our problem is to determine whether the optical field was prepared into $|0\rangle$ or $|\alpha\rangle$ using the outcome of a measurement $\hat{M}$. On the basis of the theory of quantum hypothesis testing[15], it is sufficient to consider a two-component measurement, described by the operators $\hat{M}_0$ and $\hat{M}_\alpha = \hat{1} - \hat{M}_0$, with the interpretation that one selects $|0\rangle$ when the measurement outcome corresponds to $\hat{M}_0$ and vice versa. But because coherent states are not orthogonal, quantum mechanics precludes any measurement that can discriminate perfectly between $|0\rangle$ and $|\alpha\rangle$. The ability of a given operator $\hat{M}$ to distinguish between the two states in question can be characterized using (among other information theoretic measures) the probability of error[15,16]:

$$P_{\mathrm{E}} \equiv P_M(\alpha|0)P_0(0) + P_M(0|\alpha)P_0(\alpha) \tag{1}$$

Here, $P_M\left(\psi_{i\neq j}|\psi_j\right)$ is the conditional probability based on the measurement $\hat{M}$ that one erroneously selects $|\psi_i\rangle$ when the field was actually prepared into the state $|\psi_j\rangle$. $P_M(\psi_i|\psi_j)$ is determined by the quantum measurement statistics for $\hat{M}_i$ with respect to the state $|\psi_j\rangle$: specifically, $P_M(\alpha|0) = \mathrm{tr}\left[\hat{M}_\alpha|0\rangle\langle 0|\right]$ and $P_M(0|\alpha) = \mathrm{tr}\left[\hat{M}_0|\alpha\rangle\langle\alpha|\right]$. By weighting the two incorrect decisions by the a priori likelihoods of $|0\rangle$ and $|\alpha\rangle$, P_{E} quantifies the probability that one would mis-identify the field state in any individual measurement realization. We restrict ourselves here to equal a priori likelihoods, $P_0(0) = P_0(\alpha) = 1/2$, as this reflects the least classical prior information for use in decision making. Also, without loss of generality, our analysis applies to discriminating between any two coherent states $|\psi_0\rangle$ and $|\psi_1\rangle$ by performing an unconditional displacement to $|0\rangle$ and $|\alpha = \psi_1 - \psi_0\rangle$ before measurement.

Besides being a canonical problem in quantum optics, coherent state discrimination plays a fundamental role in communication theory[15]. For information to be transmitted between parties, the data must be encoded into the state of a physical system, which is itself subject to quantum mechanics. For example, in modern telecommunications, data are often encoded into an optical field using a discrete set of coherent state amplitudes by modulating the intensity or phase of a laser[11,13,16]. Achieving quantum limited discrimination between the different states of the laser field, and thus the communication symbols, is essential to minimizing the error rate when decoding the transmitted data[12,17]. Distinguishing between weak coherent states is also important to applications of quantum information science, in particular for quantum key distribution.

To determine the optimal measurement for discriminating between coherent states, one minimizes equation (1) over all valid quantum maps. Doing so leads to the quantum limit[15,16]:

$$P_{\mathrm{QL}} = \frac{1}{2}\left(1 - \sqrt{1 - \mathrm{e}^{-\bar{n}_\alpha}}\right) \tag{2}$$

achieved by the so-called 'cat-state' measurement: $\hat{M}_0^* = |m\rangle\langle m|$ where $|m\rangle = c_0(\alpha)|0\rangle + c_1(\alpha)|\alpha\rangle$ (the optimal superposition depends on α)[15]. Unfortunately, preparing such a cat state in the laboratory is generally considered extremely difficult[17,18], so much so that it has not been accomplished in the four decades since this problem was first studied.

The standard sub-optimal approach to coherent state discrimination resorts to measuring the number operator, $\hat{n} = \hat{a}^\dagger\hat{a}$, implemented approximately in the laboratory by direct photon counting[15]. State discrimination is performed by partitioning the number operator outcomes into two projectors, $\hat{M}_0 = |0\rangle\langle 0|$ and $\hat{M}_\alpha = \hat{1} - |0\rangle\langle 0|$, because (technical imperfections aside) photon counting produces $n > 0$ only when the field was prepared into $|\alpha\rangle$. An error occurs when no photons are detected due to vacuum fluctuations in $|\alpha\rangle$. The resulting state discrimination error is known as the shot-noise error probability:

$$P_{\mathrm{SN}} = \mathrm{e}^{-\bar{n}_\alpha}/2 \tag{3}$$

where $\bar{n}_\alpha = |\alpha|^2$ is the mean photon number for $|\alpha\rangle$.

In this work we demonstrate that one can surpass shot noise and even approach the quantum limit using real-time quantum feedback[8–10] in place of the cat-state measurement. Our approach exploits the finite duration of any real measurement. In the present context, the quantum states $|0\rangle$ and $|\alpha\rangle$ are realized as optical wavepackets with spatiotemporal extent. Measurements on an optical pulse inherently

[1]Quantum Measurement & Control Group, Department of Physics and Astronomy, The University of New Mexico, Albuquerque, New Mexico 87131, USA.

persist for a time set by the pulse length, τ. For example, photon counting generates a measurement record $\Xi_{[0,\tau]} = (t_1, t_2, \ldots, t_n)$ that consists of the observed photon arrival times even if $\hat{M}$ is modelled using standard quantum measurement theory by viewing the total number of photon arrivals in the counting interval $[0,\tau]$ as one aggregate 'instantaneous' measurement of the number operator. Rather, we exploit this time to feed back on the optical field in a manner that emulates the actual cat-state measurement.

A diagram of our closed-loop measurement is shown in Fig. 1a. Following the proposal by Dolinar[13], we combine photon counting with feedback-mediated optical displacements applied during the photon counting interval. The amplitude of the displacement u_t applied at each time t during the measurement is conditional on the accumulated measurement record $\Xi_{[0,t]}$ and based on an evolving bayesian estimate of the incoming wavepacket state[13,17]. Discrimination is performed by selecting the state $|\psi\rangle \in \{|0\rangle, |\alpha|\}$ that maximizes the conditional probability $P(\Xi_{[0,t]}|\psi, u_{[0,t]})$ that the measurement record $\Xi_{[0,t]}$ would be observed given the state $|\psi\rangle$ and the history of applied displacements $u_{[0,t]}$. The feedback controller determines which state is most consistent with the accumulating record $\Xi_{[0,t]}$ and chooses the feedback amplitude at each point in time to minimize the probability of error over the remainder of the measurement interval $(t, \tau]$. The policy for determining the optimal displacement amplitude u_t^* is found by minimizing a time-additive extension of equation (1)[17]:

$$P_E[u_t] = \frac{1}{2}\int_0^\tau dt \left[P(\alpha|0, u_{[0,t]}) + P(0|\alpha, u_{[0,t]})\right] \quad (4)$$

that demands minimal error at all times during the measurement, not just in its aggregate statistics. Here, $P(\psi_i|\psi_j, u_{[0,t]})$ is the probability of selecting $|\psi_i\rangle$ given the field state $|\psi_j\rangle$ and the displacement history $u_{[0,t]}$ averaged over measurement records. Functional minimization of equation (4) was first performed by Dolinar[13] and more recently using modern optimal control theory[17]. The resulting feedback policy:

$$u_t^*(n_{[0,t)}) = \frac{\alpha}{2}\left(\frac{e^{i\pi(n_{[0,t)}+1)}}{\sqrt{1-e^{-\bar{n}_\alpha t/\tau}}} - 1\right) \quad (5)$$

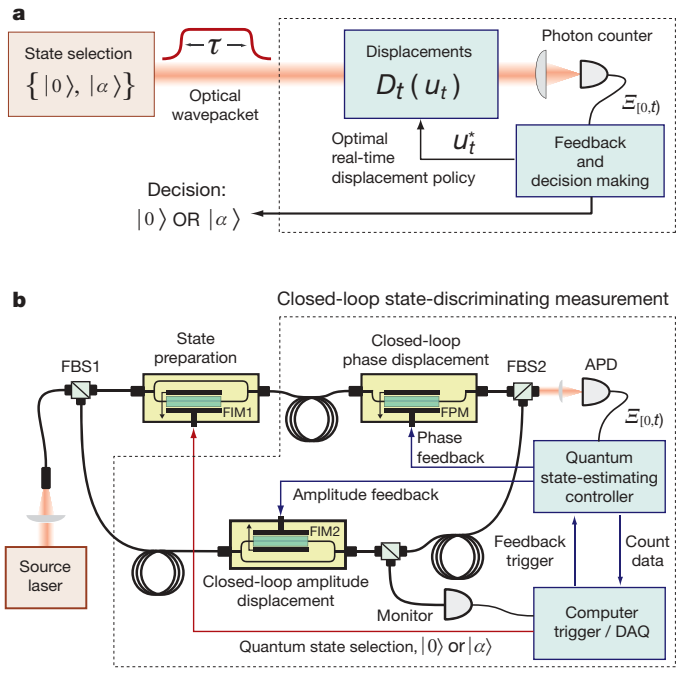

Figure 1 | Closed-loop quantum state discrimination. **a**, We consider a measurement that combines photon counting with feedback-mediated optical displacements to enact quantum-limited state discrimination between the coherent states $|0\rangle$ and $|\alpha\rangle$. **b**, A simplified diagram of our laboratory implementation of **a**. See main text for details.

with the decision procedure that $|\alpha\rangle$ ($|0\rangle$) is chosen when the number of photon counts in the measurement interval $n_{[0,\tau]}$ is even (odd), analytically achieves the fundamental quantum limit, equation (2)[13,17].

Figure 1b shows a diagram of our laboratory implementation of the closed-loop measurement just described. Light from an external-cavity grating-stabilized diode laser operating at 852 nm is coupled into a polarization maintaining (PM) fibre-optic Mach–Zender interferometer. The input beamsplitter (FBS1) provides two optical fields with a well-defined relative phase: the upper arm of the interferometer acts as the target quantum system for state discrimination and the lower arm provides an auxiliary field used to perform closed-loop displacements at the second beamsplitter (FBS2). Photon counting on the outcoupled field is implemented using a gated silicon avalanche photodiode (APD), and our feedback controller is constructed from a combination of programmable waveform generators and high-speed digital signal processing electronics (feedback bandwidth ~30 MHz). A digital counter records the number of photon counter clicks generated in each measurement interval

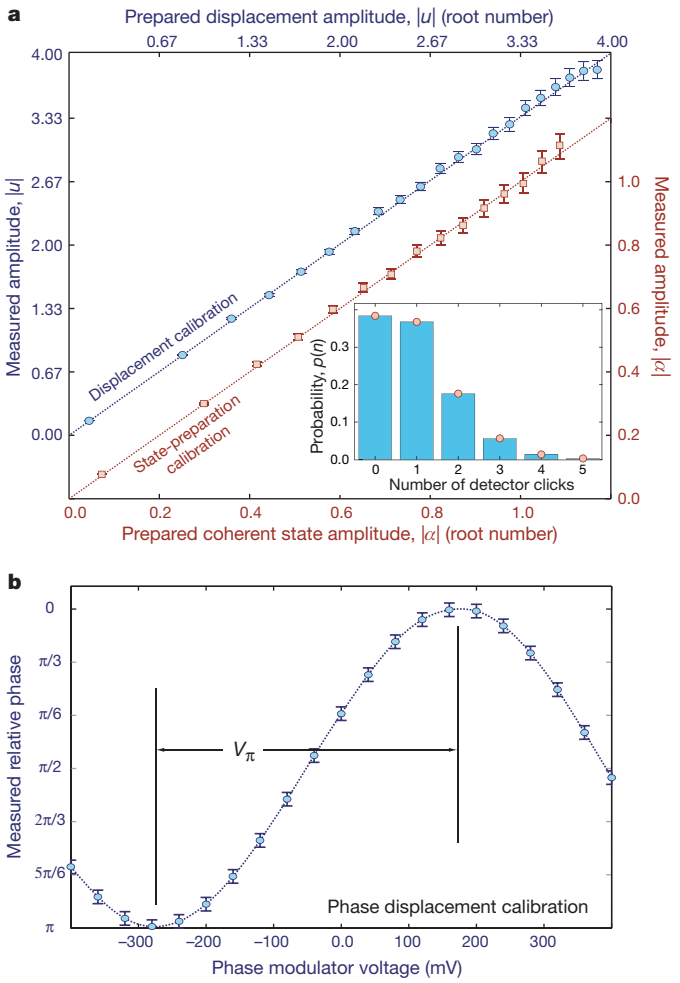

Figure 2 | State preparation and control displacement calibration. **a**, Demonstration of our ability to prepare optical coherent states (blue circles) and perform controlled displacements (red squares) with high fidelity using a precision calibration of our apparatus. Inset, a Poisson fit of our photon counting statistics for $\alpha \approx 1$, illustrating that our state preparation is quantum-limited. **b**, Demonstration of our ability to apply controlled phase displacements $\phi(u_t)$. The calibration in **b** illustrates the low control voltages (V_π) required to drive our apparatus, which allows for high-bandwidth application of the measurement feedback control. Each data point in **a** and **b** reflects a statistical ensemble of 100,000 replicate measurements, with error bars given by the estimated sample standard deviation.

$[0,\tau]$, during which the feedback controller determines the feedback amplitude, equation (5), via the accumulating count record $n_{[0,t)}$.

Coherent states for discrimination are realized as $\tau = 20\,\mu s$ optical pulses produced by a computer-controlled PM fibre-optic intensity modulator (FIM1) in the upper arm of the interferometer. The calibration parity between desired and observed values of $|\alpha|$ in Fig. 2a (red squares) highlights our ability to prepare arbitrary optical coherent states with amplitudes $0.1 \leq |\alpha| \leq 1$ (the phase of α is described below). Counting statistics for one such preparation with $\bar{n}_\alpha \approx 1$ is shown in the inset plot. The red circles in the inset are a poissonian fit to the counting data, for which we compute $\chi^2 - 1$ below 1 p.p.m., providing compelling evidence that our state preparation is quantum noise-limited. We perform a similar calibration analysis using the intensity modulator in the lower arm of the interferometer (FIM2). The amplitude in this arm is used to implement the magnitude of the control displacement $|u_t|$ applied to the target quantum state via the outcoupling beamsplitter FBS2. Figure 2a plots the parity between the desired and observed displacement amplitude $|u_t|$ (blue circles). The phase of our prepared coherent states $\phi(\alpha)$ and the phase of the feedback displacements $\phi(u_t)$ are implemented by the modulator (FPM) in the upper arm of the interferometer. Without loss of generality, we always chose $\phi(\alpha) = 0$ to simplify the interpretation of our displacements. Figure 2b illustrates our ability to control the relative interferometer phase and thus apply $\phi(u_t)$. We actively stabilize the laser intensity, interferometer path length, and modulator temperature to enable accurate comparison of different statistical ensembles. Residual technical imperfections in our experiment result primarily from detector dark counts ($\bar{n}_d = 0.0078$), interferometer phase noise ($\delta\phi \approx 8$ mrad), and finite extinction of our modulators.

With feedback disabled, our measurement reduces to direct photon counting. The data (red squares) in Fig. 3a show that, in the absence of feedback, our observed probability of error for discriminating between $|0\rangle$ and $|\alpha\rangle$ faithfully reproduces shot noise (solid red line) as a function of $\bar{n}_\alpha = |\alpha|^2$. Each data point was calculated using 100,000 optical pulses sampled randomly from $\{|0\rangle, |\alpha\rangle\}$ with equal probability. We use the label $|0\rangle$ to signify the darkest field $\bar{n}_0 \approx 0.008$ we can achieve given finite intensity-modulator extinction. The residual field appears to have a negligible effect, with a discrepancy between our photon counting data in Fig. 3a and equation (3) of $\chi^2 - 1 = 1.13 \times 10^{-5}$.

The data in Fig. 3a have been adjusted to account for finite detector efficiency and optical losses. That is to say, the coherent state amplitudes in our experiment are normalized with respect to the average photon number $\bar{n}_\alpha = |\alpha|^2$ measured by the APD over a $t = 20\,\mu s$ square-envelope pulse. Owing to the nature of coherent states, it has been shown that the detection efficiency η (resulting from the combination of detector quantum efficiency η_d and optical efficiency η_e) factors out of a comparison between the shot-noise and quantum limts[17]. For comparison, we have plotted the shot-noise error and quantum limits that would correspond to ideal detection ($\eta = 1$) in Fig. 3a. We have independently determined the intrinsic efficiency of our apparatus to be approximately $\eta \approx 0.35$.

Figure 3b, traces 1–4, shows an example closed-loop measurement trajectory in which the field was prepared into the state $|\alpha = 0.20\rangle$, to be distinguished from $|0\rangle$. The measured pulse envelope of the prepared coherent state is depicted in trace 1 and the shaded regions ($t < 0$ and $t > \imath$) indicate that the APD is gated off at those times. Before $t = 0$, the displacement amplitude is pre-established to its initial value to suppress ringing and slew-rate limitations. Careful inspection of equation (5) reveals that the optimal displacement diverges at early time, $|u_0| \to \infty$. However, finite modulator extinction (and APD saturation to a lesser extent) limits the practical maximum displacement that can be applied in trace 2. Our maximum displacement corresponds to $\bar{n}_u \approx 15.8$, although this could be increased with additional intensity modulators in future experiments.

Many aspects of the closed-loop measurement are evident from the single-shot trajectory in Fig. 3b. At $t = 0$ there is no reason to prefer one state, $|0\rangle$ or $|\alpha\rangle$, over the other. But as more data become available, the controller refines its bayesian estimate of the incoming optical state by updating the conditional probabilities $P\left(\psi|\Xi_{[0,t]}, u_{[0,t]}\right)$, described above. The premiss behind the closed-loop measurement is to displace the field to the vacuum in each shot and decide which state is present based on the displacement applied to cancel the field. As the controller gains increased confidence in its guess, it is better able to perform the correct nulling displacement. From equation (5),

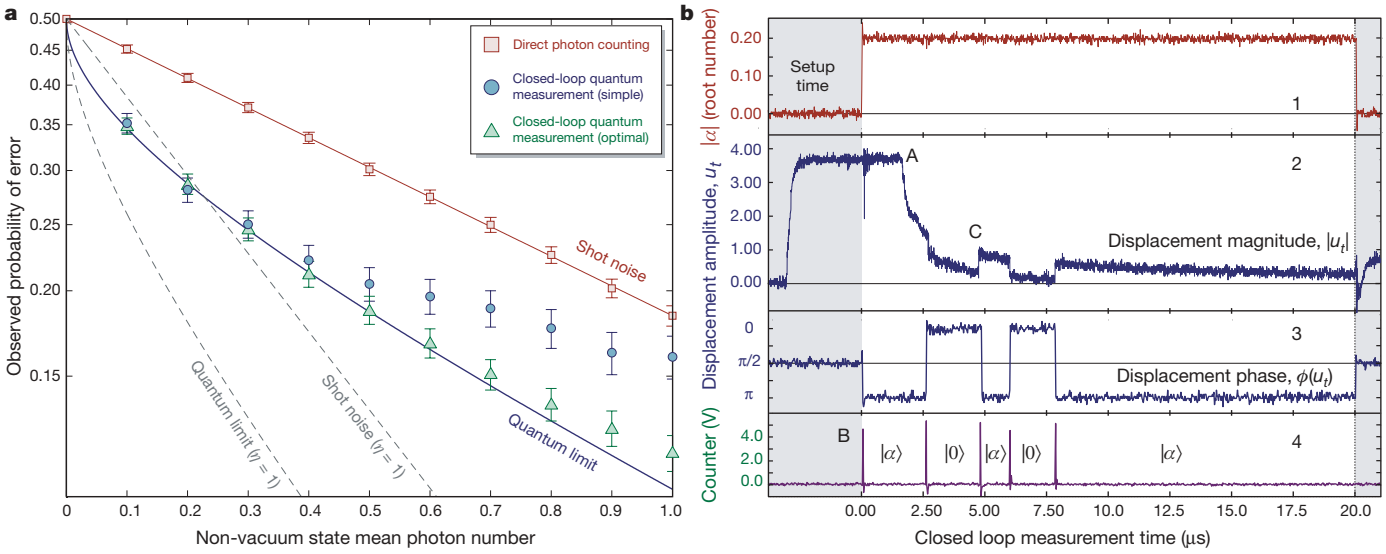

Figure 3 | Laboratory observation of sub-shot-noise state discrimination. **a**, The measured probability of error versus mean photon number for both direct photon counting (red squares) and our closed-loop measurement interpreted using a bayesian estimator that assumes application of the optimal closed-loop control policy (blue circles) and one that accounts for experimental imperfections (green triangles). All data points were obtained from ensembles of 100,000 measurement trajectories, with error bars that reflect the sample standard deviation. The four traces in **b** (1–4) depict a single-shot closed-loop measurement trajectory, discussed in detail in the text. We draw attention to several technical issues: first, the finite dynamical range of our displacements (point A on graph); second, the initial APD click is a timing signal, not a real detection event (B); and third, the apparent rise time is that of the monitor photodiode not the feedback (C).

the displacement magnitude $|u_t^*|$ is inversely proportional to the time-dependent decision uncertainty $\sqrt{1-\exp(-\bar{n}_\alpha t/\tau)}$; although not readily apparent, performing the optimization of equation (4) reveals that it is statistically optimal for the closed-loop measurement to reverse its state hypothesis with each detector click during the counting interval[13,17]. The sequence of hypothesis reversals in the example closed-loop trajectory is denoted along with the measurement record in Fig. 3b trace 4. As the measurement record accumulates, the controller eventually settles on its final (correct) decision, which in this case is $|\alpha\rangle$.

The data (blue circles) in Fig. 3a demonstrate that the closed-loop state discrimination procedure described above (alternating guesses between $|\alpha\rangle$ and $|0\rangle$ with each photon arrival) surpasses the shot-noise error probability for amplitudes $|\alpha|$ less than about one. We essentially saturate the fundamental quantum limit over a non-trivial region of parameter space $\bar{n}_\alpha < 0.3$. Performance does degrade at larger mean photon numbers owing to technical limitations: most significantly, finite extinction in the intensity modulator prevents $|u_t|$ from achieving the optimal magnitude $|u_t^*|$ at early measurement times—the contrast ratio of the modulator prevents us from inputting an arbitrarily large field into the lower arm of our interferometer (see Fig. 1) as the closed-loop displacement policy for $|0\rangle$ requires $|u_t| \approx 0$.

The data (blue circles) in Fig. 3a were determined assuming that we implemented the optimal feedback control policy in equation (5) perfectly by selecting the state $|\psi\rangle \in \{|0\rangle, |\alpha\rangle\}$ to maximize the conditional probability $P\left(\Xi_{[0,t]}|\psi, u^*_{[0,\tau]}\right)$. This approach is clearly sub-optimal owing to the technical imperfections in our control displacements just described. On the basis of a suggestion by H. M. Wiseman (personal communication; a similar approach was taken in the adaptive phase measurement)[14], we reinterpreted our raw measurement data to account for deviations between the feedback actually performed in our experiment $u_{[0,\tau]}$ and the optimum policy $u^*_{[0,\tau]}$. The data (green triangles) in Fig. 3a reflect an analysis based on the true conditional probability $P\left(\Xi_{[0,t]}|\psi, u_{[0,\tau]}\right)$, and we find that our procedure nearly achieves the quantum limit (for our detection efficiency) over the full range of coherent states we investigated. This improvement to Dolinar's original solution[13] was made possible by an optimal control theoretic treatment of coherent state discrimination[17]. We observe that even with detection efficiency $\eta \approx 0.35$ our closed-loop measurement slightly outperforms the ideal shot-noise error that would be achieved in a technically lossless experiment $\eta = 1$ for photon numbers $\bar{n} < 0.2$.

Our experiment complements previous work on adaptive quantum measurements[14,19]: rather than optimizing over a parameterized space of measurements (for example, quadrature operators) for a fixed state, our procedure manipulates the state of the observed system for a fixed measurement. Quantum feedback can be viewed as manipulating the outcome statistics of the number operator $\hat{n}$. In the absence of feedback, the detailed measurement record consisting of photon arrival times $\Xi_{[0,\tau]} = (t_1, t_2, \ldots, t_n)$ provides no more information than the total number n: Poisson processes are stationary in time, but with feedback, the significance of each click depends on when it occurs, even though the field is described by some coherent state at each point in time. The optimal feedback policy applies displacements in a manner that extracts as much information out of each photon arrival as possible. It is in this manner that we surpass shot noise to achieve the fundamental quantum limit over a non-trivial range of $|\alpha|$.

Furthermore, our procedure is evidently less demanding on the measurement resources needed to achieve optimal statistics than a direct implementation of a cat state. At no point in time do we generate a superposition between optical coherent states, yet we effectively achieve the optimal result by exploiting the time-dependence of the measurement. Our results suggest that demanding quantum resources such as entanglement and superposition states may in fact be fungible. At least here, it was possible to replace the use of such fragile resources with a more robust method—quantum feedback.

Received 14 December 2006; accepted 1 February 2007.

1. von Neumann, J. *Mathematical Foundations of Quantum Mechanics* (Princeton Univ. Press, Princeton, 1955).
2. Kraus, K. *Lecture Notes in Physics* Vol. 190, *States, Effects, and Operations: Fundamental Notions of Quantum Theory* (Springer, Berlin, 1983).
3. Peres, A. & Wooters, W. K. Optimal detection of quantum information. *Phys. Rev. Lett.* **66,** 1119–1122 (1991).
4. Fuchs, C. A. & Peres, A. Quantum-state disturbance versus information gain: Uncertainty relations for quantum information. *Phys. Rev. A* **53,** 2038–2045 (1996).
5. Nielsen, M. & Chuang, I. *Quantum Computation and Quantum Information Science* (Cambridge Univ. Press, Cambridge, UK, 2000).
6. Peres, A. Neumark's theorem and quantum inseparability. *Found. Phys.* **20,** 1441–1453 (1990).
7. Leibfried, D. *et al.* Toward Heisenberg-limited spectroscopy with multiparticle entangled states. *Science* **304,** 1476–1478 (2004).
8. Wiseman, H. M. & Milburn, G. J. All-optical versus electro-optical quantum-limited feedback. *Phys. Rev. A* **49,** 4110–4125 (1994).
9. Doherty, A. C., Habib, S., Jacobs, K., Mabuchi, H. & Tan, S. M. Quantum feedback control and classical control theory. *Phys. Rev. A* **62,** 012105–012117 (2000).
10. Geremia, J., Stockton, J. K. & Mabuchi, H. Real-time quantum feedback control of atomic spin-squeezing. *Science* **304,** 270–273 (2004).
11. Helstrom, C. W. Detection theory and quantum mechanics. *Inform. Control* **10,** 254–291 (1967).
12. Sasaki-Usuda, T. & Hirota, O. in *Quantum Communication and Measurement* (eds Belavkin, V. P., Hirota, O. & Hudson, L.) 419–428 (Plenum, New York, 1995).
13. Dolinar, S. *Quarterly Progress Report* (Tech. Rep. 111, Research Laboratory of Electronics, MIT, 1973).
14. Armen, M. A., Au, J. K., Stockton, J. K., Doherty, A. C. & Mabuchi, H. Adaptive homodyne measurement of optical phase. *Phys. Rev. Lett.* **89,** 133602–133605 (2002).
15. Helstrom, C. W. *Mathematics in Science and Engineering* Vol. 123, *Quantum Detection and Estimation Theory* (Academic, New York, 1976).
16. Fuchs, C. A. *Distinguishability and Accessible Information in Quantum Theory*. Ph.D. thesis, Univ. New Mexico (1996); ⟨http://arxiv.org/quant-ph/9601020⟩ (1996).
17. Geremia, J. Distinguishing between optical coherent states with imperfect detection. *Phys. Rev. A* **70,** 062303–062311 (2004).
18. Sasaki, M. & Hirota, O. Quantum decision scheme with a unitary control process for binary quantum-state signals. *Phys. Rev. A* **54,** 2728–2736 (1996).
19. Wiseman, H. M. Adaptive phase measurements of optical modes: Going beyond the marginal Q distribution. *Phys. Rev. Lett.* **75,** 4587–4590 (1995).

Acknowledgements We thank H. M. Wiseman, H. Mabuchi, S. Dolinar, K. Jacobs, A. Landahl, C. Caves, I. Deutsch and P. Jessen for discussions. This work was supported by the AFOSR and the New Mexico NSF EPSCoR programme in nanotechnology.

Author Contributions All authors contributed equally to this work.

Author Information Reprints and permissions information is available at www.nature.com/reprints. The authors declare no competing financial interests. Correspondence and requests for materials should be addressed to J.M.G. (jgeremia@unm.edu).